J Membrane Biol (2013) 246:131–140
DOI 10.1007/s00232-012-9511-x

Expression of Transient Receptor Potential Vanilloid Channels TRPV5 and TRPV6 in Human Blood Lymphocytes and Jurkat Leukemia T Cells

Irina O. Vassilieva · Victor N. Tomilin · Irina I. Marakhova · Alla N. Shatrova · Yuri A. Negulyaev · Svetlana B. Semenova

Received: 31 May 2012 / Accepted: 15 October 2012 / Published online: 1 November 2012

Abstract Regulation of Ca^{2+} entry is a key process for lymphocyte activation, cytokine synthesis and proliferation. Several members of the transient receptor potential (TRP) channel family can contribute to changes in $[Ca^{2+}]_{in}$; however, the properties and expression levels of these channels in human lymphocytes continue to be elusive. Here, we established and compared the expression of the most Ca^{2+}-selective members of the TRPs, Ca^{2+} channels transient receptor potential vanilloid 5 and 6 (TRPV5 and TRPV6), in human blood lymphocytes (HBLs) and leukemia Jurkat T cells. We found that TRPV6 and TRPV5 mRNAs are expressed in both Jurkat cells and quiescent HBLs; however, the levels of mRNAs were significantly higher in malignant cells than in quiescent lymphocytes. Western blot analysis showed TRPV5/V6 proteins in Jurkat T cells and TRPV5 protein in quiescent HBLs. However, the expression of TRPV6 protein was switched off in quiescent HBLs and turned on after mitogen stimulation of the cells with phytohemagglutinin. Inwardly directed monovalent currents that displayed characteristics of TRPV5/V6 currents were recorded in both Jurkat cells and normal HBLs. In outside–out patch-clamp studies, currents were reduced by ruthenium red, a nonspecific inhibitor of TRPV5/V6 channels. In addition, ruthenium red downregulated cell-cycle progression in both activated HBLs and Jurkat cells. Thus, we identified TRPV5 and TRPV6 calcium channels, which can be considered new candidates for Ca^{2+} entry into human lymphocytes. The correlation between expression of TRPV6 channels and the proliferative status of lymphocytes suggests that TRPV6 may be involved in the physiological and/or pathological proliferation of lymphocytes.

Keywords TRPV5 · TRPV6 · Patch clamp · Human T cell · Cell cycle

I. O. Vassilieva · V. N. Tomilin · I. I. Marakhova · A. N. Shatrova · Y. A. Negulyaev · S. B. Semenova (✉)
Institute of Cytology, Russian Academy of Sciences, St. Petersburg, 4 Tikhoretsky Ave., St. Petersburg 194064, Russia
e-mail: svsem@mail.cytspb.rssi.ru

Introduction

Intracellular Ca^{2+} concentration ($[Ca^{2+}]_{in}$) is a crucial second messenger responsible for linking external stimuli to contraction, proliferation and gene expression. Increased $[Ca^{2+}]_{in}$ has major consequences on downstream aspects of T-cell activation such as gene activation and lymphocyte proliferation (Negulescu et al. 1994; Crabtree 1999; Feske et al. 2001; Lewis 2001). Mitogenic stimulation leads to a rise in $[Ca^{2+}]_{in}$ due to Ca^{2+} release from internal stores and Ca^{2+} influx through Ca^{2+} channels of the plasma membrane. Elevated $[Ca^{2+}]_{in}$ via an active Ca^{2+}-calmodulin (CaM) complex promotes cell proliferation by stimulating quiescent cells to enter the cell cycle, as well as by driving proliferating cells through the cell cycle and mitosis (Berridge 1993; Luigia 1998; Lipskaia and Lompré 2004; Munaron et al. 2004). Due to the small and transient release of Ca^{2+} stores in T cells, the $[Ca^{2+}]_{in}$ increase is mainly shaped by Ca^{2+} influx. Despite tremendous effort by many laboratories, the identity of the molecules involved in controlling Ca^{2+} influx remains mysterious in T cells as well as in other nonexcitable cells.

The identification of transient receptor potential (TRP) channels in *Drosophila* retina, behaving as Ca^{2+} channels, opened new perspectives in the field (Montell and Rubin 1989). The members of this superfamily perform a wide range of functions in multiple cell types. All of these

channels are cation-selective with different relative calcium selectivity (Montell et al. 2002). Transient receptor potential vanilloid 5 and 6 (TRPV5 and TRPV6) channels form a distinct group within the superfamily of TRPs. They are calcium-selective channels which serve as apical calcium entry mechanisms in absorptive and secretory tissues (Hoenderop et al. 2001; van de Graaf et al. 2006). TRPV6 is highly expressed in the intestine, placenta and exocrine tissues, whereas TRPV5 expression is most prominent in the kidney (Hoenderop et al. 2002; den Dekker et al. 2003; Nijenhuis et al. 2003a, 2003b). Members of the TRP superfamily of cation channels have homeostatic and regulatory functions in cells, and changes in their expression may contribute to cell proliferation and malignant growth. Whereas TRPV6 channels function to maintain normal calcium homeostasis, they also seem to play a role in tumor development and progression. Specifically, TRPV6 expression is upregulated in prostate cancer and other cancers of epithelial origin, highlighting its potential as a target for cancer therapy (Peng et al. 2001; Gkika and Prevarskaya 2009).

We have previously reported that human myeloid leukemia K562 cells coexpress functional TRPV5 and TRPV6 calcium channels (Semenova et al. 2009). In the present study, TRPV5/V6 gene and protein expression and functional activity of TRPV5/V6 channels were shown in human leukemia Jurkat T cells and in human blood lymphocytes (HBLs). We found that levels of TRPV5 and TRPV6 were significantly higher in malignant cells than in quiescent lymphocytes; furthermore, the TRPV6 upregulation correlated with cell-cycle progression in mitogen-stimulated lymphocytes. These results open new perspectives on the role of TRPV6 channels in physiological responses of lymphocytes such as activation and T-cell proliferation.

Materials and Methods

Cell Isolation

Human peripheral blood lymphocytes (HBLs) were isolated from fresh venous blood of healthy volunteers by Lymphosep gradient centrifugation (MP BIOmedicals, Santa Ana, CA; 1.077 g/ml, 400 g), as described previously (Marakhova et al. 2005). After brief centrifugation ($400\times g$, 30 min), the upper layer of the opaque interface containing mononuclear cells was carefully collected and washed four times in phosphate-buffered saline (PBS) solution. Monocytes were then depleted by incubation in complete RPMI medium (RPMI-1640 supplemented with 5 % heat-inactivated human serum, AB IV Rh+) for 30 min in a 5 % CO_2 incubator at 37 °C. After depletion of adherent cells, purified cells were resuspended at a concentration of 2×10^6/ml and allowed to rest overnight in complete RPMI medium in a 5 % CO_2 incubator at 37 °C. For activation experiments, the day following isolation the cell suspension (>85 % $CD3^+$, containing $CD4^+$ and $CD8^+$ T cells) was distributed into vials (2–5 ml suspension/vial). HBLs were either left unstimulated or stimulated with 10 μg/ml phytohemagglutinin M (PHA; Sigma, St. Louis, MO). Human T cells of the leukemia line Jurkat were obtained from the Cell Culture Collection (Institute of Cytology, St. Petersburg, Russia) and maintained in RPMI medium with 10 % fetal bovine serum.

Gene Expression Analysis

Extraction of total RNA from HBLs and Jurkat cells and cDNA synthesis were done as described previously (Semenova et al. 2009). Multiplex quantitative real-time PCR was performed on the Bio-Rad (Hercules, CA) iQ5 Real-Time PCR Detection System with the use of the self-designed specific primers and TaqMan probes for target genes with succinate dehydrogenase complex, subunit A (SDHA), gene as an internal control (Iyevleva et al. 2007). All primers and probes were synthesized by Syntol (Moscow, Russia).

The primer and probe sequences used were as follows: TRPV5 (forward 5′-TCACAGAGATCGACTCCTG-3′, reverse 5′-CCTTCACTGGGGTCTGTTC-3′, probe 5′-FAM -TCTGATAAACGAGAGGCTCGCCA-BHQ1-3′, 105 bp), TRPV6 (forward 5′-ATGAGCGGGATGAGCTGTG-3′, reverse 5′-ATACTCCCGTCCGCAGATC-3′, probe 5′-FAM-CCCAGATTGTGGCCACCACGG-BHQ1-3′, 110 bp) and SDHA (forward 5′-CCACTCGCTATTGCACACC-3′, reverse 5′-CACTCCCCGTTCTCCATCA-3′, probe 5′-JOE-ACGGTC TCTGCGATATGATACCA-BHQ-3′, 102 bp). Thermal cycling parameters were 95 °C for 10 min and then 48 cycles of denaturation (95 °C, 20 s) and annealing/elongation (63 °C, 60 s). All reactions were performed in triplicate at a minimum. The threshold cycle (C_t) numbers of SDHA were stable across samples ($C_t = 23.8 \pm 0.7$). ΔC_t values were calculated in every sample for each target gene as follows: $C_{t\ \text{target}} - C_{t\ \text{SDHA}}$.

Western Blot Analysis

Cells were incubated in lysis buffer (0.5 % Nonidet P-40, 150 mM NaCl, 10 mM NaF, 1 mM Na_3VO_4, 50 mM Tris–HCl, pH 7.6, and protease inhibitor cocktail; Sigma) for 15 min on ice, and then the suspension was gently homogenized. After centrifugation for 10 min at $10{,}000\times g$, the supernatant was collected and the protein concentration determined. Cell lysates were boiled for 5 min in Laemmle buffer. Then, 20 μg/lane of protein in

sample buffer were separated by SDS-PAGE (8 % gel) and analyzed by Western blot. Western blotting was performed as previously described (Semenova et al. 2009). Primary antibodies were anti-TRPV5 (Santa Cruz Biotechnology, Santa Cruz, CA; K-17), anti-TRPV6 (Alomone Labs, Jerusalem, Israel) and anti-β-actin (Sigma-Aldrich, St. Louis, MO; A5316). Visualization was carried out using horseradish peroxidase-conjugated secondary antibodies (Sigma), enhanced chemiluminescence (ECL) reagents (Amersham, Aylesbury, UK) and exposure to X-ray film. Blots were scanned and densitometry was performed with ImageJ (http://imagej.nih.gov/ij).

Electrophysiology and Data Analysis

At the beginning of the experiment, Jurkat cells or HBLs were plated on poly-L-lysine-coated glass coverslips. The recording chamber (volume 0.1 ml) was filled with divalent-free (DVF) external solution in which a gigaseal was formed. Single-channel currents were recorded using the standard outside-out mode of the patch-clamp technique. We used a micropipette puller P-97 (Sutter Instrument, Novato, CA) to manufacture patch pipettes with a resistance of 8–15 MΩ when filled with solution. Membrane currents were measured using an Axopatch 200B patch-clamp amplifier (Axon Instruments/Molecular Devices, Eugene, OR), low-pass-filtered at 1 kHz and digitized at 5 kHz with an A/D converter. Data were collected and analyzed with pClamp software (Axon Instruments/Molecular Devices). Membrane voltage was calculated as the potential of the intracellular membrane side minus the potential of the extracellular one. Recordings were performed at room temperature (22–23 °C) on the stage of an inverted microscope with Nomarsky optics. Data analysis was performed using Microcal Origin 6.2 software (OriginLab, Northampton, MA). Data are presented as means ± SE; n = number of experiments. Error bars are shown where they exceed the symbol size. The patch pipette solution in outside–out mode contained (in mM) 140 K-aspartate or Cs-aspartate, 5 NaCl, 10 HEPES/TrisOH, 10 BAPTA and 10 D-glucose (pH 7.3). The bath solution contained (in mM) 140 Na-methanesulfonate, 5 KCl, 10 HEPES/TrisOH, 10 HEDTA and 10 D-glucose (pH 7.3). All chemicals were from Sigma-Aldrich.

Cell-Cycle Analysis

Resting and PHA-treated HBLs and Jurkat cells (5×10^5 cells/ml) were incubated for 48 h in the presence or absence of ruthenium red (RR, 50 μM), then harvested, pelleted by centrifugation and resuspended in PBS. One-half of each sample was subjected to cell-cycle analysis and the other half to cell viability assessment. For cell-cycle analysis, 0.2 mg/ml saponin (Fluka, Buchs, Switzerland), 0.05 mg/ml propidium iodide (Sigma) and 0.25 mg/ml RNAse (Sigma) were added to each sample tube and incubated for 30 min at 37 °C. Cellular DNA content was analyzed by flow cytometry using the EPICS XL Flow Cytometer (Beckman Coulter, Brea, CA) equipped with an argon laser (15 mW) emitting at 488 nm. A total of 15,000–20,000 cells were analyzed in each sample. Cells were classified as G_0/G_1, S and G_2/M. List mode files were analyzed with ModFitLT (Verity Software House, Topsham, ME).

Cell Viability Assessment

Propidium iodide (PI) exclusion was used to determine cell viability after drug treatment. PI (0.05 mg/ml) was added to the samples just before analysis, mixed gently and analyzed by flow cytometry (Beckman Coulter). Each sample was analyzed for 50 s, the sample flow rate was set to high (60 μl/min) and at least 20,000 cells were acquired for analysis. Triplicate counts were obtained for each procedure.

Results

TRPV5 and TRPV6 mRNA and Protein Expression in Quiescent HBLs and Jurkat T Cells

TRPV5 and TRPV6 expression was studied at the mRNA and protein levels in quiescent HBLs and Jurkat T cells. To evaluate the relative amount of TRPV5 and TRPV6 transcripts, we performed real-time PCR analysis. The comparative ΔC_t method with housekeeping gene SDHA as internal control (the higher the ΔC_t value, the lower the initial target cDNA content) had shown that TRPV5 ΔC_t values were lower in Jurkat cells (7.7 ± 0.1, $n = 3$) than in resting HBLs (10.16 ± 1.02, $n = 8$). TRPV6 ΔC_t had a wide distribution in HBLs (7.8–13.8, $n = 8$); however, in six of eight HBL samples TRPV6 ΔC_t values revealed a significant reduction (11.9 ± 1.06, $n = 6$) in comparison with Jurkat cells (9.5 ± 0.12, $n = 3$). In general, data from real-time PCR showed that expression of both TRPV5 ($n = 8$) and TRPV6 ($n = 6$) was significantly lower in quiescent HBLs (Fig. 1a) than in Jurkat cells ($p < 0.05$).

Western blot analysis detected TRPV5 and TRPV6 proteins in Jurkat cells as immunoreactive doublets at ~75 and 85–100 kDa (Fig. 1b). The immunoreactive protein bands at 75 kDa reflected the core protein, while the presence of the other TRPV5 and TRPV6 immunoreactive bands at 100 kDa suggested posttranslational modification (Hoenderop et al. 2003). The presence of TRPV5 protein

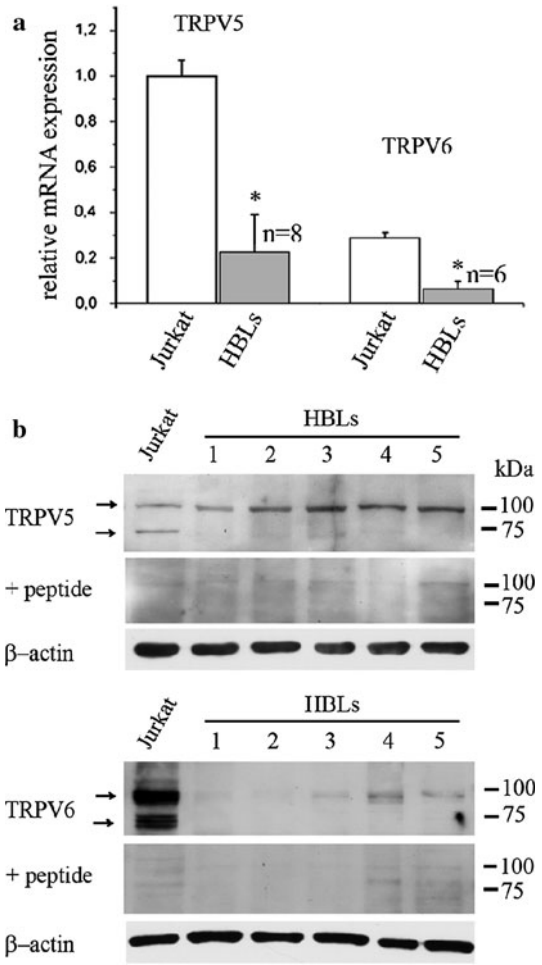

Fig. 1 TRPV5 and TRPV6 mRNA and protein expression in Jurkat cells and in quiescent HBLs. **a** TRPV5 and TRPV6 mRNA levels were measured by real-time RT-PCR. Expression levels of the target mRNAs were normalized to SDHA and reported relative to the value of TRPV5 in Jurkat cells (the highest value) by the formula $2^{-\Delta\Delta Ct}$, where $\Delta\Delta C_t = (C_t \text{ target} - C_t \text{ SDHA})_{sample} - (C_t \text{ TRPV5} - C_t \text{ SDHA})_{Jurkat}$. These experiments were performed in triplicate. Data are expressed as mean ± SD, where $^*p < 0.05$ according to Student's *t* test. **b** Representative Western blot analysis of whole-cell extracts from Jurkat cells and resting HBLs. Jurkat cells and HBLs obtained from five healthy donors (*lanes* 1–5) were lysed, and a constant amount of proteins (20 μg/lane) was separated by SDS-PAGE. Membranes were probed with polyclonal antibodies directed against TRPV5 or TRPV6, respectively. *Arrowheads* indicate specific bands. The specificity of primary antibodies was confirmed by blotting the membranes with anti-TRPV5 or anti-TRPV6 preincubated with a corresponding blocking peptide (*+peptide*), following the manufacturer's instructions. The loading control was β-actin (42 kDa) (*bottom panels*)

($n = 8$) was also assessed in quiescent HBLs as one immunoreactive band with a molecular size of 100 kDa (Fig. 1b). In contrast, the level of TRPV6 protein was low or undetectable ($n = 8$) in quiescent HBLs (Fig. 1b). It should be noted that in two HBL samples that exhibited a high level of TRPV6 mRNA the protein was not detected by the TRPV6-specific antibody.

Upregulation of TRPV6 in Mitogen-Stimulated HBLs

HBLs have been employed extensively as a model system for investigating the regulation of the initial stages of cellular proliferation and entry into the cell cycle. Normal human T lymphocytes can proliferate in culture for a few days when activated with mitogenic lectin PHA. To investigate a possible link between TRPV5 and TRPV6 expression and the proliferative status of cells, quiescent HBLs were activated for 48 h with 10 μg/ml PHA. Flow-cytometric analysis performed on quiescent HBLs confirmed that the great majority (99 %) of these cells were in the G_0/G_1 phase of the cell cycle (Fig. 2a). However, after 48-h treatment with PHA, lymphocytes entered the mitotic cycle and >37 % of the cells progressed from G_0/G_1 to S and G_2/M phases.

We compared TRPV5 and TRPV6 protein expression in quiescent HBLs and in HBLs stimulated with PHA for 4, 8, 24 and 48 h. Immunoblot analysis revealed no change in TRPV5 content between quiescent and PHA-treated cells ($n = 8$). In contrast, a significant increase of nonglycosylated (75 kDa) and glycosylated (~100 kDa) forms of TRPV6 protein was detected in lymphocytes stimulated for 24–48 h (Fig. 2b). Densitometric analysis showed a 5.5-fold enhancement ($p < 0.05$, $n = 8$) of TRPV6 in PHA-treated HBLs compared with resting cells (Fig. 2c). Thus, while TRPV6 protein was faintly expressed in resting blood cells, its synthesis and maturation were upregulated as soon as the cells were induced to enter the proliferative cycle.

TRPV5/V6 Channel Activity in Outside–Out Patches from HBLs and Jurkat T Cells

Recently, using 140 mM Na^+ as a charge carrier and DVF solution, we discovered TRPV5 and TRPV6 channels in human myeloid leukemia K562 cells (Semenova et al. 2009). In this study, typical channels were detected in Jurkat cells and normal HBLs. In the majority of the experiments, step-like increases in the current were frequently detected during outside-out recording in DVF solution. Figure 3a shows inwardly directed unitary currents recorded in the plasma membrane of K562 cells, Jurkat cells and resting HBLs. All-points amplitude histograms constructed from the currents displayed multiple peaks representing the activity of more than one channel. The average unitary current amplitudes calculated from all-points amplitude histograms were identical in K562 cells (1.88 ± 0.05 pA at −70 mV, $n = 15$), Jurkat cells (2.3 ± 0.1 pA at −70 mV, $n = 11$) and HBLs (2.0 ± 0.1 pA at −70 mV, $n = 8$). Single-channel recordings over a broad potential range revealed no detectable channel activity at membrane potentials more positive than −20 mV

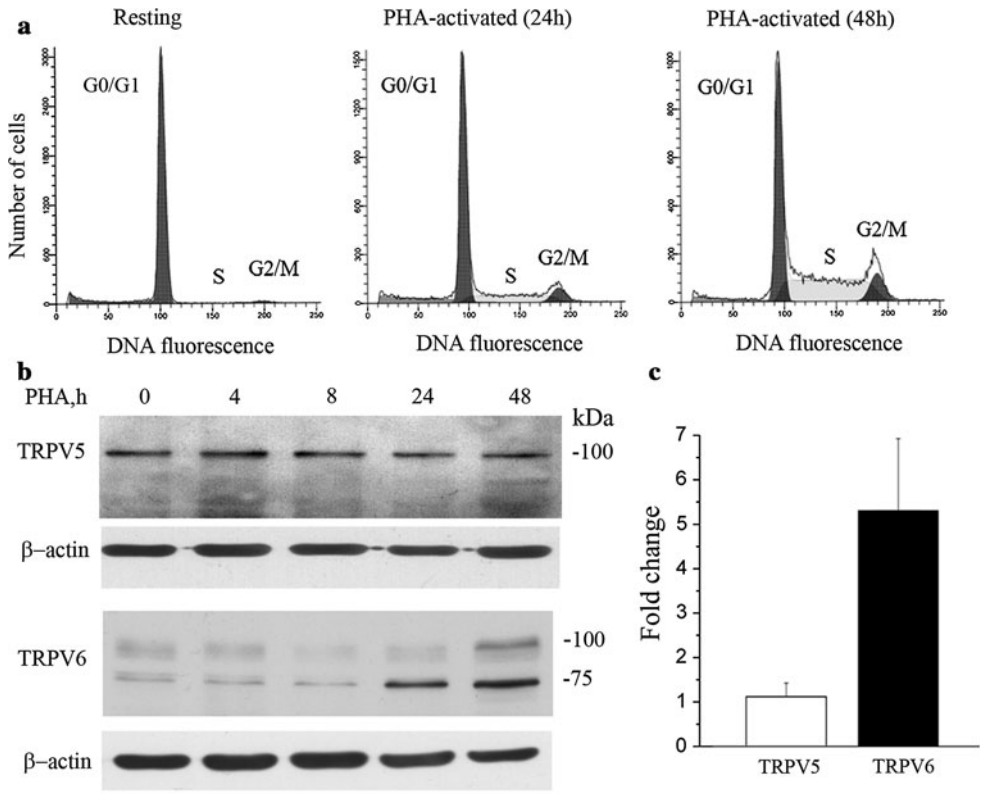

Fig. 2 Cell-cycle progression and TRPV5/V6 protein expression in phytohemagglutinin (PHA)–treated HBLs. **a** Representative result of flow-cytometric analysis on HBLs. Quiescent cells and lymphocytes stimulated with PHA (10 μg/ml) were examined for DNA content using propidium iodide staining, as described in Materials and Methods. **b** Representative Western blots showing TRPV5 and TRPV6 protein content in resting and PHA-treated HBLs. Both resting cells and HBLs stimulated with PHA (for 4, 8, 24 and 48 h) were lysed, and a constant amount of protein (20 μg/lane) was resolved by SDS-PAGE. Blots were probed with polyclonal antibodies directed against TRPV5 and TRPV6 proteins, respectively. The loading control was β-actin (42 kDa) (*bottom panels*). **c** Normalized TRPV5/β-actin and TRPV6/β-actin protein ratios from PHA-treated (for 24 h) samples were compared with the corresponding normalized values of resting lymphocytes (set as 1) and expressed as a fold increase. Data are expressed as mean ± SEM, $n = 8$, where $^*p < 0.05$ according to Student's t test

(Fig. 3b). *I–V* relationships displayed a strong inward rectification with extrapolated reversal potential in the vicinity of 0 mV (Fig. 3c). The slope unitary conductance determined from the *I–V* relationships in the range of negative potentials averaged 38 ± 0.3 pS ($n = 11$) for Jurkat cells and 36 ± 0.2 pS ($n = 6$) for HBLs.

From an electrophysiological point of view, TRPV5 and TRPV6 are highly homologous channels. They can be discriminated, however, by their sensitivity to RR as TRPV6 has a 100 times lower affinity for RR (IC_{50} 10 μM) than TRPV5 (IC_{50} 130 nM) (Hoenderop et al. 2001). Here, we tested the effects of RR on the activity of endogenous channels in Jurkat cells. Figure 4 shows representative single-channel recordings before and after addition to the external solution of different concentrations of RR. The recordings were made in outside-out patches at a holding potential of −70 mV. The channels recorded in T cells displayed different sensitivities to RR. In several experiments 0.5–1 μM RR caused complete inhibition of inward monovalent currents (Fig. 4a) and channels had a sensitivity similar to that previously reported for recombinant TRPV5 channels (IC_{50} 190 ± 9.3 nM, $n = 7$) (Fig. 4b). Besides, we also recorded the channels that had a 100-fold lower affinity to RR than TRPV5. These channels had a sensitivity similar to that of recombinant TRPV6 ($IC_{50} = 8.5$ μM ± 1.5 nM, $n = 6$) and were completely inhibited by 20–50 μM RR (Fig. 4c, d).

RR Inhibits Cell-Cycle Progression in Human Lymphocytes

As was shown above, TRPV6 upregulation correlated with cell-cycle progression in mitogen-stimulated lymphocytes. Therefore, we examined the possible involvement of TRPV6 channels in lymphocyte proliferation. Here, RR was used as the most effective inhibitor of TRPV6 channels. HBLs were stimulated with PHA and incubated for 48 h with or without 50 μM RR. Then, the cell-cycle phase distribution in cells was measured by flow-cytometric

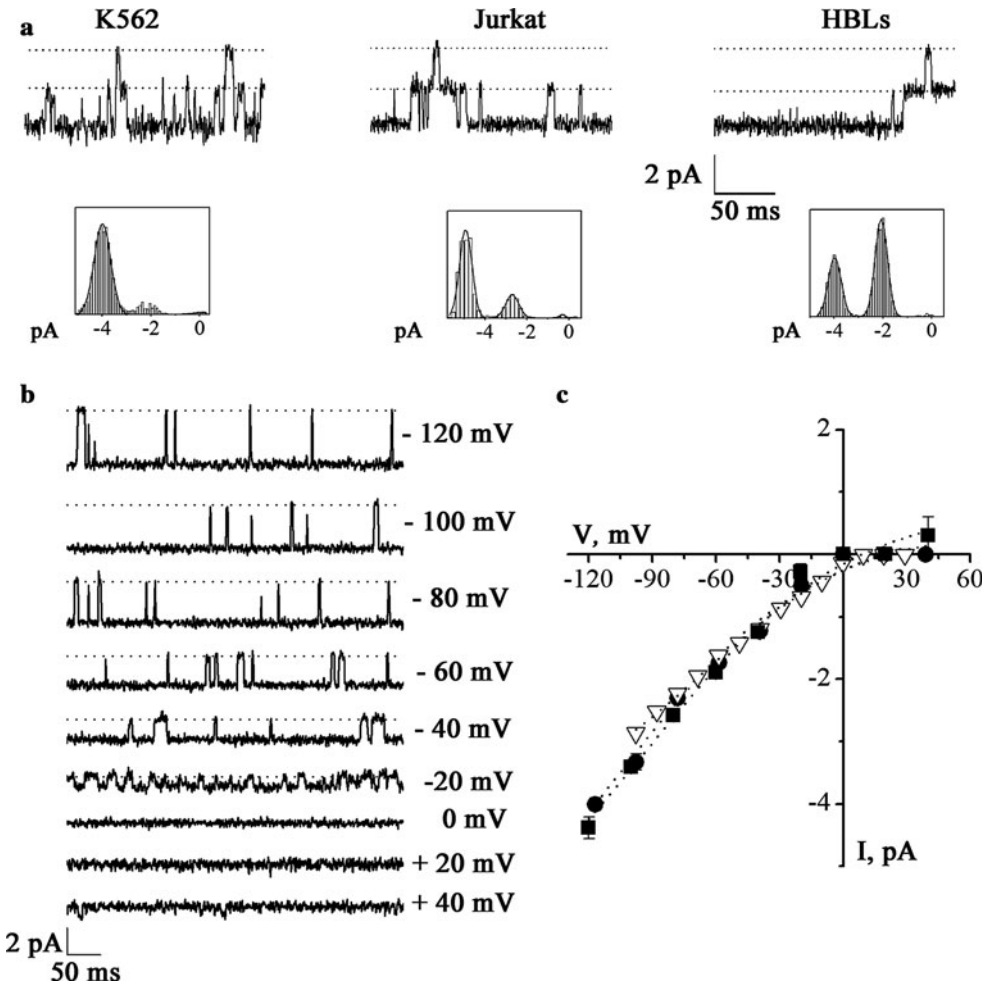

Fig. 3 Activity of TRPV5/V6 channels in plasma membrane of blood cells recorded in divalent-free solutions. **a** Single-channel currents recorded in outside–out patches in K562, HBL and Jurkat cells. Membrane potential is −70 mV. All-points amplitude histograms of the currents display three peaks, which correspond to the open and closed states of the channels. **b** Inward rectification of unitary currents recorded in Jurkat cells at membrane potentials indicated near each trace. *Dashed lines* correspond to the closed state of the channel. Current–voltage (*I–V*) relationships of unitary currents recorded in K562 cells (*open triangles*), Jurkat cells (*filled squares*) and HBLs (*filled circles*). Each point is a mean ± SEM from 4–15 patches. Estimated channel unitary conductance is 30 pS for K562 cells, 36 pS for HBLs and 38 pS for Jurkat cells

analysis (FACS). Figure 5a demonstrates that incubation of lymphocytes with RR results in reduction of PHA-induced cell-cycle progression. Percentages in S and G_2/M phases for activated lymphocytes decreased from 28.9 to 11.8 % for cells in the absence and presence of RR, respectively.

In addition, we tested the effect of RR on cell-cycle progression in Jurkat cells. A standard number of cells per milliliter of liquid culture (5×10^5) were incubated for 48 h with or without 50 μM RR and then subjected to FACS analysis. As shown in Fig. 5b, after 48 h of exposure to RR, the percentage of Jurkat cells in S phase did not differ from the nontreated control; however, the percentage of cells in G_2/M increased nearly 1.8-fold (from 13.6 ± 0.4 to 24.0 ± 0.9). FACS analysis revealed that RR affected the proliferation of Jurkat cells by arresting them in the G_2/M phase of the cell cycle. Figure 5c demonstrates that RR (for 48 h) at a concentration that fully blocked the TRPV5/V6 current significantly (by 16 %; $p < 0.05$, $n = 4$) decreased the number of Jurkat cells compared with control cells. According to our data 50 μM RR did not reduce the cell number by causing significant cell death and was not toxic for cells.

Discussion

The data presented here demonstrate TRPV5 and TRPV6 gene expression, protein expression and functional activity of TRPV5/V6 calcium channels in leukemia Jurkat T cells and HBLs. In recent years, several members of the TRP channel family have been identified in human lymphocytes; however, most of the studies have been carried out on transformed cells, and few data are available from primary lymphocytes. Expression of TRPV5 and TRPV6 mRNAs was previously reported in Jurkat T cells using RT-PCR or Northern blot analysis (Cui et al. 2002). However, expression of these channels in normal human leukocytes was not found by Northern blot analysis (Wissenbach et al. 2001). Here, we report that HBLs express both TRPV6 and TRPV5 mRNAs; however, the levels of these mRNAs were significantly lower in quiescent HBLs than in leukemia T cells.

In most studies, mRNA, but not protein, expression is analyzed. This allows comparison of only the global mRNA in cells, while the effects of translational regulation, posttranslational processing and protein degradation

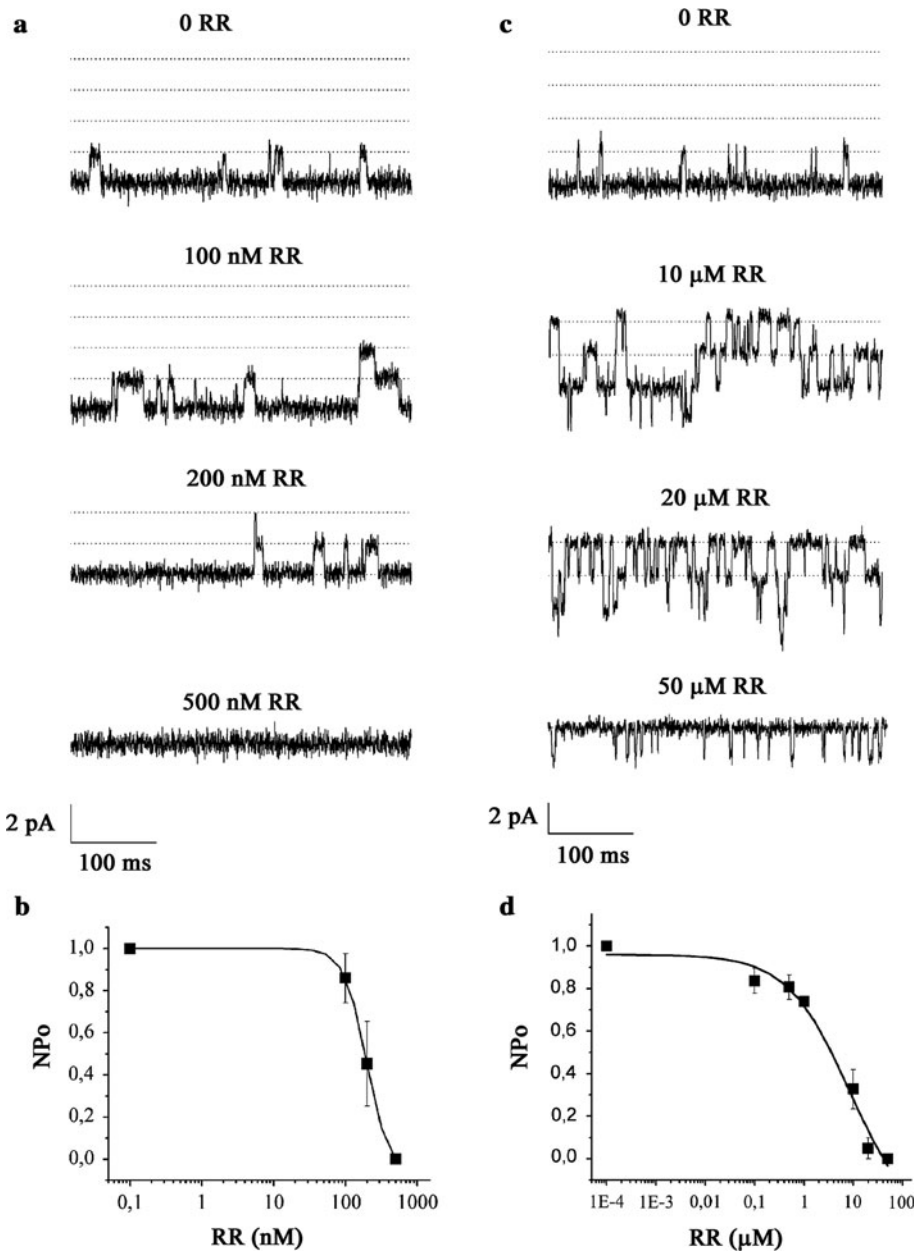

Fig. 4 Inhibition of TRPV5/V6 channels activity in Jurkat cells by ruthenium red (*RR*). Unitary currents recorded in two independent outside–out patches before and after addition of different concentrations of RR. **a** RR (500 nM) completely inhibited TRPV5 channel activity in Jurkat cells. **b** NP_O as a function of extracellular RR concentration. NP_O at each RR was normalized to *NP*o at 0 RR. Each point represents the mean ± SEM of 5–7 measurements from different patches. *Continuous line* represents the logistic fit of experimental data. The IC_{50} value for RR block was 190 ± 9.3 nM. **c** RR (50 µM) completely inhibited TRPV6 channel activity in Jurkat cells. **d** NP_O as a function of extracellular RR concentration. NP_O at each RR was normalized to *NP*o at 0 RR. Each point represents the mean ± SEM of 4–6 measurements from different patches. *Continuous line* represents the logistic fit of experimental data. The IC_{50} value for RR block was 8.5 µM ± 1.5 nM. The pipette solution in outside-out mode contained 140 mM K-aspartate/10 mM BAPTA. Bath solution contained 140 mM Na^+ methanesulfonate/ 10 HEDTA. Membrane potential was –70 mV

are ignored. Here, in addition to mRNA studies, we analyzed TRPV5 and TRPV6 protein expression in both normal human lymphocytes and leukemia T cells. We found differences in TRPV5 mRNA expression but not in TRPV5 protein content between resting HBLs and leukemia T cells. In contrast, TRPV6 mRNA and protein levels were both significantly lower in quiescent HBLs than in leukemic cells. It is worthy of note that membrane proteins can show a discordant correlation between mRNA transcript and protein levels; for example, in chronic lymphocytic leukemia, although there was good correlation between gene and protein expression of CD19, CD20, CD23 and CD138 cell surface markers, other proteins including immunoglobulin light chain, CD38 and CD79b showed no correlation between gene and protein expression (Zent et al. 2003).

We found that TRPV6 protein is poorly expressed in resting lymphocytes; however, its synthesis and maturation are upregulated during cell progression from quiescence to proliferation in mitogen-stimulated HBLs. Indeed, HBLs enter the S and G_2/M phases as soon as 24 h after PHA treatment, and TRPV6 protein level is significantly increased at that time. These results indicate that TRPV6 upregulation is associated with increased proliferative activity in leukemic cells and in activated lymphocytes. Our results are in agreement with data showing elevated expression of TRPV6 in colon, breast, thyroid, ovarian and pancreatic carcinomas in comparison with normal tissues

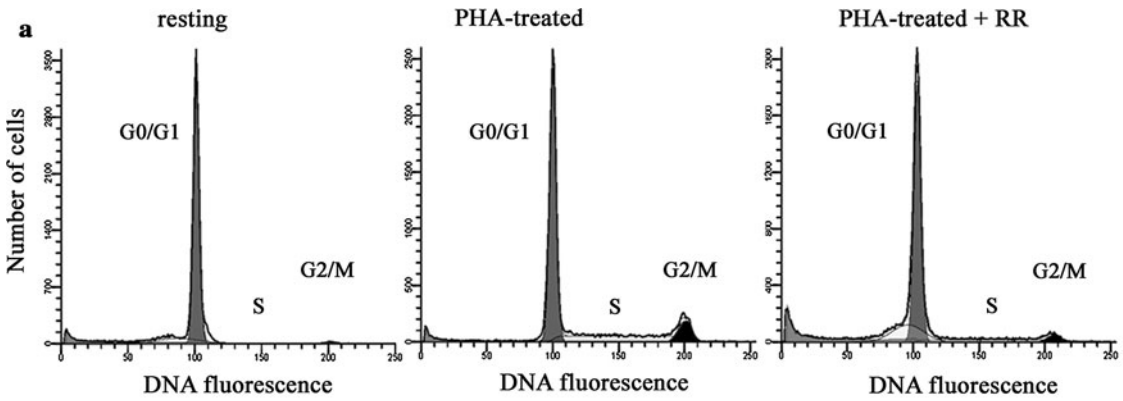

n = 3	G0/G1	S	G2/M
resting HBLs	97.6±0.8	1.2 ± 0.9	1.1 ± 0.1
PHA-treated HBLs	71.1 ±6.1	18.9 ± 4.4	10.0 ± 1.8
PHA-treated HBLs (+50 μM RR)	88.1±3.8	8.5 ± 3.5	3.3 ± 0.5

Cell cycle (%)

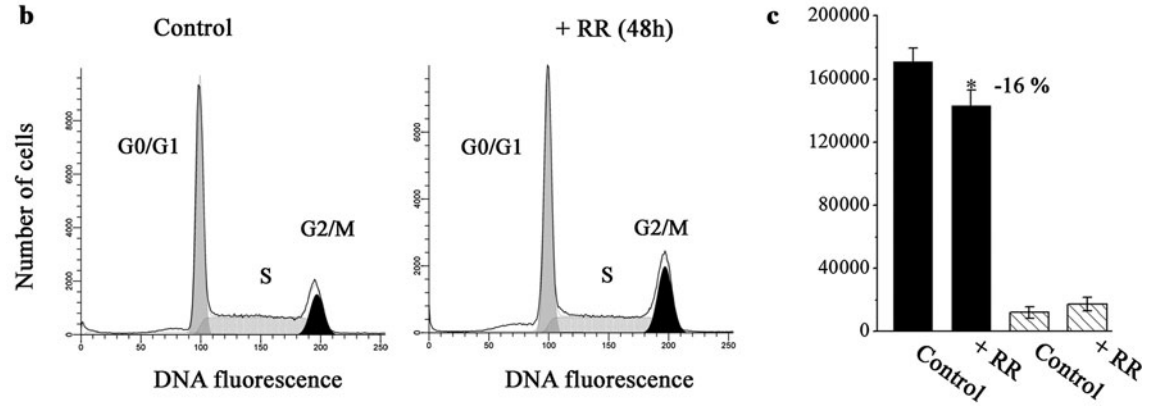

n = 3	G0/G1	S	G2/M
Jurkat	50.3 ± 3.4	36.06 ± 3.0	13.6 ± 0.4
Jurkat (+50 μM RR)	39.9 ± 2.8	36.0 ± 1.8	24.0 ± 0.9

Cell cycle (%)

Fig. 5 Ruthenium red (*RR*) decreases cell-cycle progression in phytohemagglutinin (PHA)–treated lymphocytes and Jurkat cells. **a** Flow-cytometric histograms of propidium iodide-labeled HBLs. Quiescent cells and HBLs stimulated with PHA (10 μg/ml) were incubated for 48 h in the presence or absence of RR (50 μM) and subjected to FACS analysis. **b** Flow-cytometric histograms of propidium iodide–labeled Jurkat cells. Jurkat cells were incubated in the presence or absence of RR (50 μM) for 48 h and subjected to FACS analysis. **c** Data represent the average number of live cells (*filled columns*) and dead cells (*hatched columns*) from three separate experiments. Bars marked "Control" represent Jurkat cells that had been allowed to proliferate for 48 h in drug-free growth medium. Control data were then compared with cells incubated for 48 h with 50 μM RR. Cell-cycle analysis was performed as reported in Materials and Methods. The number of viable cells was determined by propidium iodide exclusion. $*p < 0.05$ compared with control

(Peng et al. 2001; Gkika and Prevarskaya 2009). Also, several studies (Schwarz et al. 2006; Lehen'kyi et al. 2007) have reported that Ca^{2+} input through TRPV6 channels modulates proliferation of transformed cells and changes their resistance to apoptotic death. It is worth noting that no change in TRPV5 protein content was revealed between quiescent and PHA-treated cells. TRPV5 and TRPV6 channels share a high degree of amino acid identity (74 %) and have several functional properties in common (van de Graaf et al. 2006). Despite this very close relationship,

TRPV5 was not reported to be linked to cell proliferation or cancer progression.

Our previous investigation on human myeloid leukemia K562 cells demonstrated 30-pS channels that were activated by removing extracellular divalent ions. The monovalent currents in K562 cells displayed kinetic and pharmacological characteristics of unitary TRPV5/V6 currents. The channel recordings presented here revealed the presence of ~36-pS cation channels in HBLs and ~38-pS cation channels in Jurkat cells in DVF solution. Monovalent currents through these channels displayed a strong inward rectification. Previously, similar 30- and 40-pS monovalent channels were described during whole-cell recording in T cells and RBL-2H3 cells (Fomina et al. 2000; Braun et al. 2001; Prakriya and Lewis 2002), which were believed to be endogenous TRPM7 channels. However, strong inward rectification was not typical for TRPM7 currents. Outward currents via recombinant TRPM7 channels were readily recorded in cell-attached and inside-out patches (Runnels et al. 2001, 2002). In contrast, we have not observed single-channel activity at positive voltages during continuous recordings in K562 cells, Jurkat cells or HBLs in DVF solution. Our results suggested that endogenous currents detected in human lymphocytes were unlikely to be mediated via TRPM7 channels.

Single-channel properties described in the present study resembled properties of TRPV5 and TRPV6 calcium channels. The strong inward rectification of monovalent currents in blood cells was similar to that described for currents via expressed TRPV6/V5 channels (Hoenderop et al. 2001; Voets et al. 2003; Yue et al. 2001). The single-channel conductance (36–38 pS) for monovalent cations in lymphocytes was close to that reported for TRPV5/V6 (Nilius et al. 2000; Yue et al. 2001). We found that a potent blocker of TRPV5/V6, RR, blocked single-channel activity in human lymphocytes. Moreover, the affinities for RR (IC_{50} ~190 nM and ~8.5 μM) in T cells were similar to those previously reported for recombinant TRPV5 (IC_{50} ~130 nM) and TRPV6 (IC_{50} ~10 μM) channels (Hoenderop et al. 2001). In whole, a strong inward rectification of the currents, the close range of single-channel conductance and the sensitivity of the channels to RR resembled biophysical and pharmacological properties of the recombinant TRPV5/V6 channels. Overall, our electrophysiological and biochemical data strongly indicate that calcium channels TRPV5 and TRPV6 are expressed in HBLs.

It should be noted that in expression systems TRPV5 and TRPV6 channels could function as homo- or heterotetramers (Hoenderop et al. 2003). Heterotetrameric TRPV5/6 proteins displayed properties that, depending on the subunit configuration, are intermediate between TRPV5 and TRPV6. It was previously reported that replacing TRPV5 by TRPV6 subunits in the heterotetrameric channel had major effects on the block by RR (Hoenderop et al. 2003). Different sensitivity of the channels to RR in lymphocytes may reflect the different compositions of heterotetrameric TRPV5/6 complexes. Variations in subunit composition of TRPV5/6 channels define the channel properties, thus affecting the intracellular calcium regulation. Hence, regulation of the relative expression levels of TRPV5 and/or TRPV6 may affect the Ca^{2+} transport kinetics and Ca^{2+}-dependent functions, such as proliferation and differentiation, in human blood cells.

Elevated $[Ca^{2+}]_{in}$ is an important stimulus driving lymphocyte proliferation under both physiological and pathological conditions. Despite this, the plasma membrane channels responsible for mitogen-activated calcium entry remain an elusive family of proteins. We showed here widespread expression of TRPV6 in leukemia cells but not in quiescent HBLs. Moreover, TRPV6 protein is upregulated during cell progression from quiescence to proliferation in mitogen-stimulated HBLs. In addition, we showed that the proliferative potential of stimulated HBLs and exponentially growing Jurkat T cells can be drastically reduced through TRPV6 inhibition. In whole, these data suggest a regulatory role of TRPV6 channels in normal and/or pathological lymphocyte proliferation. However, further studies are needed, especially in order to understand the relationship between TRPV6 channel expression/activity and proliferative activity of lymphocytes.

Acknowledgements The authors are grateful to Drs. Viktor Kharazia (Ernest Gallo Clinic and Research Center, University of California) and Nevin Mlodik (Medical College of Wisconsin) for critical reading and correcting of this article. This work was supported by grants from the Russian Foundation for Basic Research (11-04-01030) and the Molecular and Cell Biology Program of the Russian Academy of Sciences.

References

Berridge MJ (1993) Inositol trisphosphate and calcium signalling. Nature 361:315–325

Braun FJ, Broad LM, Armstrong DL, Putney JW (2001) Stable activation of single Ca^{2+} release-activated Ca^{2+} channels in divalent cation-free solutions. J Biol Chem 276:1063–1070

Crabtree GR (1999) Generic signals and specific outcomes: signaling through Ca^{2+}, calcineurin, and NF-AT. Cell 96:611–614

Cui J, Bian JS, Kagan A, McDonald TV (2002) CaT1 contributes to the stores-operated calcium current in Jurkat T-lymphocytes. J Biol Chem 277:47175–47183

den Dekker E, Hoenderop JGJ, Nilius B, Bindels RJM (2003) The epithelial calcium channels, TRPV5 and TRPV6: from identification towards regulation. Cell Calcium 33:497–507

Feske S, Giltnane J, Dolmetsch R, Staudt LM, Rao A (2001) Gene regulation mediated by calcium signals in T lymphocytes. Nat Immunol 2:316–324

Fomina AF, Fanger CM, Kozak JA, Cahalan MD (2000) Single channel properties and regulated expression of Ca^{2+} release-activated Ca^{2+} (CRAC) channels in human T cells. J Cell Biol 150:1435–1444

Gkika D, Prevarskaya N (2009) Molecular mechanisms of TRP regulation in tumor growth and metastasis. Biochim Biophys Acta 1793:953–958

Hoenderop JGJ, Vennekens R, Müller D, Prenen J, Droogmans G, Bindels RJM, Nilius B (2001) Function and expression of the epithelial Ca^{2+} channel family: comparison of mammalian ECaC1 and 2. J Physiol 537:747–761

Hoenderop JGJ, Nilius B, Bindels RJM (2002) Molecular mechanism of active Ca^{2+} reabsorption in the distal nephron. Annu Rev Physiol 64:529–549

Hoenderop JGJ, Voets T, Hoefs S, Weidema F, Prenen J, Nilius B, Bindels RJM (2003) Homo- and heterotetrameric architecture of the epithelial Ca^{2+} channels TRPV5 and TRPV6. EMBO J 22:776–785

Iyevleva AG, Buslov KG, Togo AV, Matsko DE, Filimonenko VP, Moiseyenko VM, Imyanitov EN (2007) Measurement of DPD and TS transcripts aimed to predict clinical benefit from fluoropyrimidines: confirmation of the trend in Russian colorectal cancer series and caution regarding the gene referees. Onkologie 30:295–300

Lehen'kyi V, Flourakis M, Skryma R, Prevarskaya N (2007) TRPV6 channel controls prostate cancer cell proliferation via Ca^{2+}/NFAT-dependent pathways. Oncogene 26:7380–7385

Lewis RS (2001) Calcium signaling mechanism in T lymphocytes. Annu Rev Immunol 19:497–521

Lipskaia L, Lompré AM (2004) Alteration in temporal kinetics of Ca^{2+} signaling and control of growth and proliferation. Biol Cell 96:55–68

Luigia S (1998) The role of calcium in the cell cycle: facts and hypotheses. Biochem Biophys Res Commun 244:317–324

Marakhova I, Karitskaya I, Aksenov N, Zenin V, Vinogradova T (2005) Interleukin-2-dependent regulation of Na/K pump in human lymphocytes. FEBS Lett 579:2773–2780

Montell C, Rubin GM (1989) Molecular characterization of the drosophila trp locus: a putative integral membrane protein required for phototransduction. Neuron 2:1313–1323

Montell C, Birnbaumer L, Flockerzi V (2002) The TRP channels, a remarkably functional family. Cell 108:595–598

Munaron L, Antoniotti S, Fiorio Pla A, Lovisolo D (2004) Blocking Ca^{2+} entry: a way to control cell proliferation. Curr Med Chem 11:1533–1543

Negulescu PA, Shastri N, Cahalan MD (1994) Intracellular calcium dependence of gene expression in single T lymphocytes. Proc Natl Acad Sci USA 91:2873–2877

Nijenhuis T, Hoenderop JGJ, Nilius B, Bindels RJM (2003a) (Patho)physiological implications of the novel epithelial Ca^{2+} channels TRPV5 and TRPV6. Pfluegers Arch 446:401–409

Nijenhuis T, Hoenderop JGJ, van der Kemp AW, Bindels RJM (2003b) Localization and regulation of the epithelial Ca^{2+} channel TRPV6 in the kidney. J Am Soc Nephrol 14:2731–2740

Nilius B, Vennekens R, Prenen J, Hoenderop JGJ, Bindels RJM, Droogmans G (2000) Whole-cell and single channel monovalent cation currents through the novel rabbit epithelial Ca^{2+} channel ECaC. J Physiol 527:239–248

Peng JB, Zhuang L, Berger UV, Adam RM, Williams BJ, Brown EM, Hediger MA, Freeman MR (2001) CaT1 expression correlates with tumor grade in prostate cancer. Biochem Biophys Res Commun 282:729–734

Prakriya M, Lewis RS (2002) Separation and characterization of currents through store-operated CRAC channels and Mg^{2+}-inhibited cation (MIC) channels. J Gen Physiol 119:487–508

Runnels LW, Yue L, Clapham DE (2001) TRP-PLIK, a bifunctional protein with kinase and ion channel activities. Science 291: 1043–1047

Runnels LW, Yue L, Clapham DE (2002) The TRPM7 channel is inactivated by PIP2 hydrolysis. Nat Cell Biol 4:329–336

Schwarz EC, Wissenbach U, Niemeyer BA, Strauss B, Philipp SE, Flockerzi V, Hoth M (2006) TRPV6 potentiates calcium-dependent cell proliferation. Cell Calcium 39:163–173

Semenova SB, Vassilieva IO, Fomina AF, Runov AL, Negulyaev YA (2009) Endogenous expression of TRPV5 and TRPV6 calcium channels in human leukemia K562 cells. Am J Physiol 296: 1098–1104

van de Graaf SFJ, Hoenderop JGJ, Bindels RJM (2006) Regulation of TRPV5 and TRPV6 by associated proteins. Am J Physiol 290:1295–1302

Voets T, Janssens A, Prenen J, Droogmans G, Nilius B (2003) Mg^{2+}-dependent gating and strong inward rectification of the cation channel TRPV6. J Gen Physiol 121:245–260

Wissenbach U, Niemeyer BA, Fixemer T, Schneidewind A, Trost C, Cavalié A, Reus K, Meese E, Bonkhoff H, Flockerzi V (2001) Expression of CaT-like, a novel calcium-selective channel, correlates with the malignancy of prostate cancer. J Biol Chem 276:19461–19468

Yue L, Peng JB, Hediger MA, Clapham DE (2001) CaT1 manifests the pore properties of the calcium-release-activated calcium channel. Nature 410:705–709

Zent CS, Zhan F, Schichman SA, Bumm KH, Lin P, Chen JB, Shaughnessy JD (2003) The distinct gene expression profiles of chronic lymphocytic leukemia and multiple myeloma suggest different anti-apoptotic mechanisms but predict only some differences in phenotype. Leuk Res 27:765–774